Protection of Patient Identity and Privacy using Vascular Biometrics

C. Lakshmi Deepika cldeepika@yahoo.com
Department of Biomedical Engineering
PSG College of Technology
Coimbatore -641004, India.

Dr. A. Kandaswamy hod@bme.psgtech.ac.in
Department of Biomedical Engineering
PSG College of Technology
Coimbatore -641004, India.

C. Vimal vimalc@ieee.org
Department of Biomedical Engineering
PSG College of Technology
Coimbatore -641004, India.

Abstract

Biometric systems are being used in hospitals to streamline patient registration and identification, as an effective measure to protect patient privacy and prevent identity theft. Many Hospitals and Healthcare institutions are turning towards Vascular Biometrics which complements the biometric recognition with hygiene and improved accuracy. In this paper, a multimodal hand vein system and a multibiometric fingerprint-hand vein biometric system are proposed. The multimodal hand vein system is a non-invasive, contactless and fast system, which uses two different feature sets extracted from each hand vein image. The multibiometric system captures both the fingerprint as well as the hand vein of the patient and hence offers even more improved performance though the speed and the cost of the system as well as the hygiene are reduced. We have used the Euclidean classifier to calculate the performance rates namely the False Rejection Rate (FRR) and False Acceptance Rate (FAR) of the Vein System and the Fingerprint-Vein System. We have performed this analysis using a volunteer crew of 74 persons. The FRR and FAR were 0.46% and 0.7% in the former case and 0% and 0.01% in the latter case respectively. The multimodal or the multibiometric system could be used based of the Hospital's requirements.

Keywords: Fingerprint, Vein, Biometrics, Fusion, Multimodal, Multi-biometric, FRR, FAR

1. INTRODUCTION

Today Biometric technology is spreading everywhere including hospitals. Biometrics is more accurate than names and numbers for collecting patient records. Some of the biometric identifiers include fingerprints, voice, face, and iris scans in physiological biometrics, and signatures, gait, keystroke dynamics in behavioral ones. These human traits possess the properties, such as universality, uniqueness, permanence, collectability, acceptability, and circumvention. Universality means that the particular biometric should be present for everyone universally and uniqueness

means that it should be unique to every person, even for identical twins. Permanence means that it should not change with time and Collectability means that it should be possible to acquire the biometric easily using simple electronic instruments and Circumvention means that it should not be possible to imitate or fake the particular biometric. A Face Recognition system is sensitive to illumination, pose and facial expressions of the subject. Facial accessories can also be easily spoofed by a static photo / moving video and further remain alike for identical twins. Hand Geometry is not very distinctive and cannot be used to identify an individual from a large population. The accuracy and speed of iris recognition systems are very high, but the cost and the amount of user participation required are also high [2, 3]. Fingerprint is a very popular biometric which is known for its high accuracy, ease of integration and low costs. Fingerprint scanners and processing algorithms are available in plenty. Though fingerprint is a universally accepted technology, one leaves traces of fingerprint everywhere and hence it can be easily traced and used to spoof the biometric system. Damage of fingerprint is common for people who do lot of manual work. Further fingerprint requires the user to put his finger in contact with the sensor. This results in dirt and moisture on the scanner which will then give noisy images. Vein Pattern is the network of blood vessels beneath the skin and this pattern is believed to be unique to every individual. Any part of the human body can be used for personal identification; however the hand veins are preferred since they are very close to skin and easily accessible. The hand vein biometric has scored very well in all the tests of the International Biometric Group (IBG) and according to Mr.Victor Lee, Senior Consultant at the International Biometric Group, vein patterns are really unique. The veins are present beneath the skin and overrule the possibility of an intruder obtaining access to it. Further vein patterns are not damaged or obscured by cuts, wounds or diseases. Vein pattern acquisition is a contact less technology and hence is more hygienic. The fingerprint and hand vein structures are randotypic traits, which form during the early phases of the embryonic development and are unique to identical twins and even to the left and right hands of the same person.

Currently, biometric systems are being used in hospitals to streamline patient registration and identification, as an effective measure to protect patient privacy and prevent identity theft. Hospitals are interested in implementing Vein biometric systems as they provide a way to identify patients who arrive unconscious at the emergency room. According to the IBG, Vein is the only biometric on par with the iris scans in terms of accuracy, which is of significant importance in hospitals to avoid mismatch between the patient and the medical record. Further vein recognition does not require any contact with the scanner and hence does not raise an issue with germs or bacteria. With several healthcare companies stepping into Vein biometrics, research in the same is gearing up. We wanted to measure the performance score of the vein pattern biometric, which is presented in this paper along with a detailed analysis of the same. We acquired the vein images using a low cost near IR camera. The morphological features in the form of bifurcations (branches) and terminations (endings) also called the minutiae were extracted from the vein images. A feature vector was created by concatenating the spatial coordinates of the positions of the minutia points. This was called the template, which is nothing but the representation of the particular biometric trait used for storage and further comparison. To test the uniqueness of the hand vein, it was necessary to acquire more number of images. Since we were not able to identify any publicly available hand vein database, we created our own database with a volunteer crew of 74 persons belonging to various age groups and both the gender [4]. It was noticed that the vein image obtained from a person at one instance may not be the same at another instance due to imperfections of producing the hand for acquisition such as rotation, scaling and translation. So the vein image was obtained for each person at ten different instances. Templates were generated for all the 740 images and tested to find out whether they were unique by a simple means, namely cross correlation, as a first step before going in for rigorous pattern matching. But from the cross correlation plot, it could be observed that the uniqueness was not very high. This could be attributed to the loss of details in vein images due to the low cost imaging setup. It was also necessary to fix a benchmark with popularly used biometric systems to assess the performance of hand veins. Since fingerprint is a very popularly used biometric, we compared the randomness of the hand veins with the fingerprints of the same person. For this a similar database with the same volunteer crew was created using the Verifinger Fingerprint acquisition

device. Fingerprint templates were created using similar fingerprint minutia points. A cross correlation plot between fingerprint templates was drawn. On comparing the vein and fingerprint plots, the fingerprints were found to be more unique than the hand veins for the given imaging setups of both the biometric identifiers. So to increase the randomness of the hand vein feature vector, we created one more feature vector by extracting the statistical data namely the moments from the hand vein images and fused this second feature vector with the first one which was created based on the morphology of the veins. Now the hand vein system is called multimodal. We again compared the randomness of the new vein template with that of the fingerprint template. It was noticed that the randomness of the fused hand vein feature vector was much higher than that of the fingerprint. So we proceeded to assess the performance by using two parameters namely the FAR (False Acceptance Rate) and FRR (False Rejection Rate). The rate of accepting the fake user (imposter) is called FAR and the rate of rejecting the genuine user as an imposter is called FRR. In this paper we have used the Euclidean Distance Classifier to classify a user as a genuine user or as an imposter. We obtained an FRR and FAR of 0.46% and 0.7% respectively for the multimodal hand vein templates. We also found out the performance of the fingerprint and the FRR and FAR were 4.81% and 2.07% respectively. Thus the Hand Vein system scores well in the various features of an ideal biometric system namely, non-invasiveness, contactless, speed and accuracy.

The experiment was extended to see if there was a further improvement in accuracy if a multibiometric system was used. Hence we fused the feature vectors of the fingerprint and hand vein templates and used the same distance based classifier to find the FRR and FAR. They were found to be 0% and 0.01% respectively. There is no biometric technology which would be equally suitable and feasible universally. The choice of the biometric system depends on the application and the environment. Hence we propose the hand vein system with fused morphological and statistical feature sets as an effective biometric system where the factors of hygiene, anti-spoof, cost-effectiveness and speed are more important. In an application where the utmost accuracy is required, a multibiometric system has to be used. The rest of the paper is organized as follows: Section II deals with Vein Image Acquisition, Section III with Vein Image Processing, Section IV with Fingerprint Image Acquisition, Section V with Fingerprint Image Processing, Section VI with Evaluation of the Multimodal System and Section VII with Evaluation of the Multibiometric System. The conclusions are provided in Section VIII.

2. VEIN IMAGE ACQUISITION

Vein Pattern Recognition is relatively an unexplored area in Biometrics and hence no public database is available. To validate our proposed fusion method, we have created a database of vein images of 74 individuals. Blood vessels are present beneath the skin and hence are not visible to the human eyes or the conventional cameras, which are sensitive to light only in the wavelengths 400 –700nm. The imaging techniques used to capture vascular images are X-rays, Ultrasonic Imaging and Infrared Imaging. Infrared Imaging is a non-invasive contact less technique and hence is preferred over the others. There are two IR imaging technologies, the Near IR and Far IR Imaging. The Far-IR imaging technique captures the thermal patterns emitted by the human body. This thermal profile is unique even to identical twins. Near IR cameras on the other hand capture radiation in the range 800 – 1100 nm of the electromagnetic spectrum. The experiments conducted by Wang Lingu and Graham Leedam [9] show that Near IR imaging is comparatively less expensive and also gives good quality vein images. They have also found that Near IR imaging is more tolerant to environmental and body conditions and provides a stable image. ZhongBo Zhang et al [10], Junichi Hashimoto et al[11] use Finger Vein Patterns. However since the hand veins are bigger, we use the veins at the back of the hand. Lin and Fan [12] use the palm veins, captured by an Infracam, a high cost IR camera.

We propose a relatively low cost imaging setup using a WAT 902H near IR camera. With our setup, we found that when the fist is clenched, the veins appear more prominent in the captured image rather than the veins in the palm. Hence we have captured the vein pattern at the back of the hand. According to Medical Physics, the hemoglobin in blood is sensitive to light in the

wavelength range of 800 – 1100 nm and absorbs the same. Hence the blood vessels in the superficial layer of the body appear dark compared to the other parts of the hand. The WAT 902H is a monochrome CCD camera. To increase the sensitivity of the capturing setup, an IR filter of 880 nm wavelength is mounted in front of the camera lens. An unexposed Ektachrome color film served effectively as an IR filter. An IR source consisting of IR LEDs was used to illuminate the back of the hand [13-18]. The output of the camera which is an analog signal is transferred to the computer using a PIXCI frame grabber. Ten images were obtained from each of the 74 individuals. A database of 740 images was thus created. The acquisition was done in a normal office environment at room temperature. The skin colors of the subjects varied from fair to dark. The distribution of the age of the subjects varied from 21 years to 55 years. The images were obtained for both the gender. It was observed that age, gender and skin colors do not play any role in the clarity of the vein image obtained.

The failure to enroll rate which measures the proportion of individuals for whom the system is unable to generate templates was found to be 0.1%. Fig 1 shows the Image Acquisition setup we have used to capture Vein Images. The user has to place his hand in the 'hand placement area' with the fist clenched.

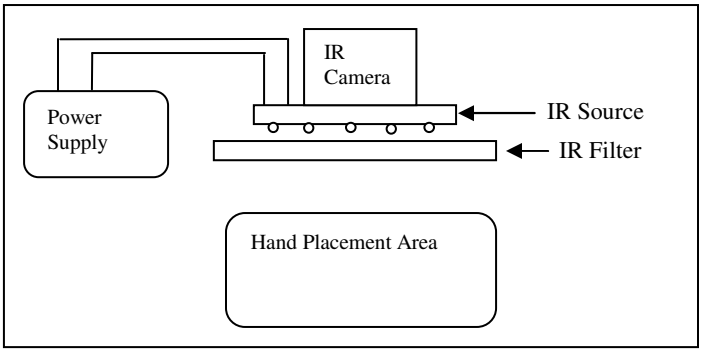

FIGURE 1: Outline of the Image Acquisition Setup

We observed that acquired vein images are independent of skin color and unique to both the left and right hands. The Acquisition setup used in our system is a low cost setup. The WAT 902H camera is a low cost camera compared to cameras like the Thermal Tracer, Infracam, etc. Also, we have fabricated our own LED power source whose radiation is also well within the acceptable limits, namely 5,100 Watts/sq.m..The IR filter we have used is easily and cheaply available than the conventional IR filters such as the Hoya filters.

3. VEIN IMAGE PROCESSING AND FEATURE EXTRACTION

The captured raw vein image has unwanted details such as hair, skin, flesh and bone structures. The image is also contaminated with noise due to extraneous lighting effects and sensor noise. Hence, before extracting the morphological features, pre-processing is done as shown in Fig 2.

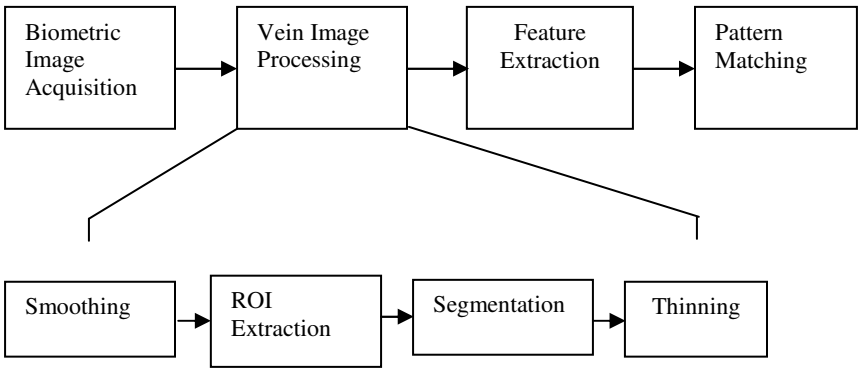

FIGURE 2: Entire Setup

3.1 Smoothing

Noise introduces high frequency components in the image. Median filter is popularly used to remove noise [14,17-18]. We propose an anisotropic diffusion process similar to the physical diffusion process where the concentration balance between the molecules depends on the density gradient. In anisotropic diffusion, for the given image u(x,y,t), the diffusivity 'g' depends on the gradient as shown in (1)

$$\begin{aligned} g &\rightarrow 0 \ for \ |\nabla u| \rightarrow \infty \\ g &\rightarrow 1 \ for \ |\nabla u| \rightarrow 0 \end{aligned} \qquad (1)$$

We have calculated the gray value of each pixel iteratively depending on the gray value gradient in a 4-pixel neighborhood surrounding the pixel. The gradient is calculated using the non-linear diffusion function 'g' so that the smoothing is more over the homogenous regions rather than the edges, so that the edges remain sharp. The noisy and noiseless images are shown in Fig 3.

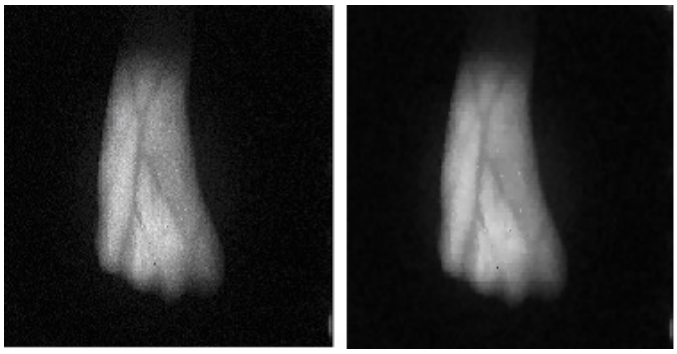

FIGURE 3: Noisy and Noiseless Images

3.2 ROI Selection

We propose an iterative method to extract the ROI. The hand image is binarised to extract its outline as shown in Fig 4(a). Horizontal and Vertical scans are done to assess the size of the image as the size differs from person to person. A rectangle is generated and centered on a window. The size of the rectangle, which depends on its length and breadth, is altered in accordance with the size of the hand by altering an amplification factor. The portion of the hand inside the rectangle is extracted as the region of interest as seen in Fig 4(b) and further in Fig 5(a).

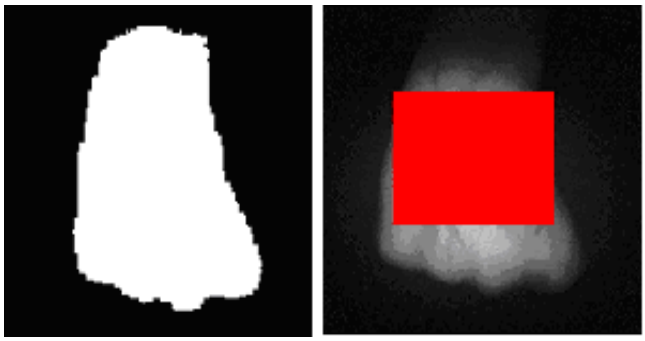

FIGURE 4: (a) Binarised hand image **(b)** ROI Selection

3.3 Segmentation

Ling u Wang et al and Kejun Wang et al [19] use a local dynamic threshold based segmentation process where the threshold is determined for each pixel by examining an r x r neighborhood of each pixel. In order to reduce the complexity by reducing the number of times the threshold is calculated, we propose a histo-threshold based segmentation to extract the vein structure from the background of the flesh and skin. It is seen that the gray level intensity values of the vein image vary at different locations of the image. Hence different threshold values are chosen for different gray levels in the image. The gray levels available in the image are extracted from the histogram of the image. The thresholds chosen are 0, 255 and all minima extracted from the histogram. This method reduces the number of thresholds determined and hence the complexity of the segmentation process.

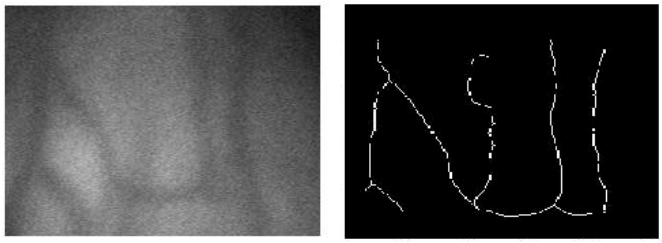

FIGURE 5: (a) ROI **(b)** Thinned Image

3.4 Thinning

The segmented vein image is skeletonised by a morphological operation called thinning. Fig 5(b) shows the thinned image, where the veins have shrunk to a minimally connected stroke. Then the operator “spur” is used to remove the end points of lines without allowing objects to break apart.

Now, it is required to extract the so called minutia points which are nothing but the bifurcations and terminations in the vein image. Kejun Wang et al [19] have extracted the endpoints and cross points from vein images similar to the extraction of minutiae points in a fingerprint image. However this method is a extensive process due to additional process of removing false minutiae. We propose to extract the corners in the vein image as suggested by Sojka [8]. He defines a corner as an intersection of two straight non-collinear gray value edges. Let ‘Q’ be an image point and let Ω be its certain neighborhood. The probability ‘P’ of any point ‘X’ lying in Ω having the same brightness as ‘Q’ is calculated. Let g(X) be the size of the brightness gradient and $\varphi(X)$ represent the direction of the brightness gradient at ‘X’. Let w(r(X)) be a weight function that represents the distance between ‘Q’ and ‘X’ as seen in (2).

$$W = \sum_{X_i \in \Omega} P(X_i) w(r(X_i)) \qquad (2)$$

$$\mu_{\varphi} = \frac{1}{W} \sum_{X \in \Omega} P(X_i) w(r(X_i) \varphi(X_i) \quad (3)$$

$$\sigma_{\varphi}^{2} = \frac{1}{W} \sum_{X_i \in \Omega} P(X_i) w(r(X_i))[\varphi(X_i) - \mu_{\varphi}]^2 \quad (4)$$

The image points for which the size of the gradient of brightness is greater than a predefined threshold (we have fixed it to be 30) are considered to be the candidates for the corners. The minutiae points have a structure as seen in Fig 6. The distances between the points are calculated and are shown in Table 1.

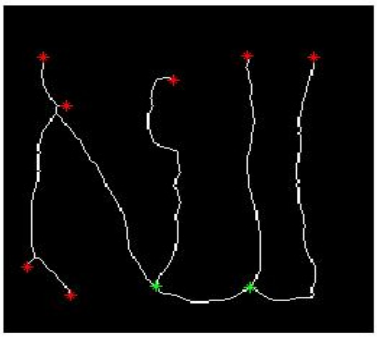

FIGURE 6: Minutia Points of Veins

9.0091	18.6605	25.9185	34.1359	36.3658
45.5350	46.8286	48.1460	61.7604	62.7712
92.1861	100.9359	103.0000	108.4836	116.7833
122.3319	125.3357	128.5756	130.9969	131.5991
133.8963	145.2548	148.9285	153.0000	163.9538

TABLE 1: Distances between Minutia points

The graph in Fig 7 shows the distribution of minutia points for 5 persons. It can be seen that they are well apart and unique to each person.

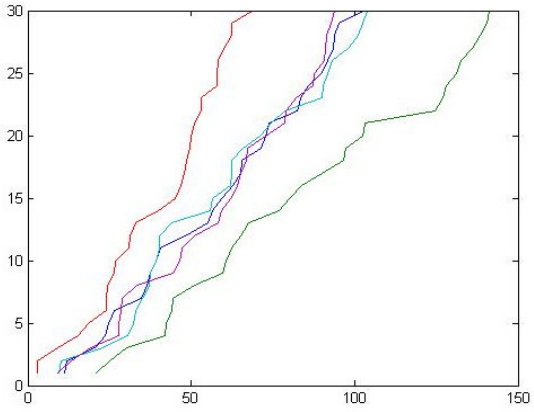

FIGURE 7: Endpoint and cross point distances for 5 persons

The minutia points are concatenated to form the feature vector. The uniqueness of the templates (feature vectors) of different persons decides to a large extent the accuracy of a biometric system. Hence to find out how far apart the feature vectors are, we picked up some samples and estimated the cross correlation between them which is seen in Fig 8. The plot in Fig 8 does not help to arrive at any conclusion. By and large, fingerprint is one of the ancient and still popular biometric used all over the world. Fingerprint scanners and processing algorithms are available in plenty. Hence we wanted to compare the randomness of the hand veins with that of the fingerprint.

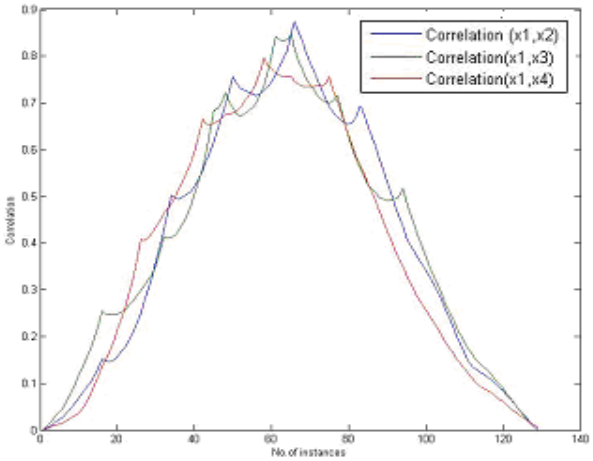

FIGURE 8: Cross Correlation Plot of Hand Vein

4. FINGER IMAGE ACQUISITION

"Verifinger" fingerprint scanner shown in Fig 9 was used to scan and digitize the images of the right thumbs of the subjects. The subjects were advised to present only the right thumb to maintain consistency and to give only the necessary pressure on the sensor since too much of pressure would create distorted and noisy images. The sensor was interfaced to the computer to transfer the fingerprint images for further processing.

FIGURE 9: Fingerprint Scanner

The Fingerprints in the database had variations among themselves since the skin dryness, oiliness and roughness varied for each person.

FIGURE 10 (a): Fingerprint with multiple cuts

While most of the images were clear, some people had multiple cuts and sometimes wide cuts in both the left and right thumb and hence were not able to enroll in the database at all.

FIGURE 10 (b): Fingerprint with wide cuts

These cuts result in loss of efficiency compared to clear images as shown in Fig 10(c)

FIGURE 10 (c): Clear Fingerprint Image

4. FINGERPRINT PROCESSING

The fingerprint images obtained from the scanner have ridges and furrows. The parts of interest are the bifurcations (branches on ridges) and terminations (endings of ridges). The dirt or residual remains on the scanner can result in noise. A simple gaussian filter was sufficient to remove noise. The image also had several broken ridges. Hence rigorous enhancement was needed before further processing.[6] The image was repaired by using Fast Fourier Transform (FFT). The FFT was performed on small sized blocks of 32x32 pixels as seen in (5).

$$F(u,v) = \sum_{x=0}^{M-1} \sum_{y=o}^{N-1} f(x,y) \exp\{-j2\Pi \left[\frac{ux}{M} + \frac{vy}{N} \right]\} \quad (5)$$

Where u = 0, 1…31 and v = 0,1,…31. M,N = size of the image. f = input image, F=FFT image. The FFT of each block is multiplied by its magnitude a set of times, in order to boost the dominant frequencies in each block. The enhanced image is obtained by taking the Inverse Fourier Transform of the product as seen in (6).

$$g(x,y) = F^{-1}\{F(u,v) \mid F(u,v) \mid^k \quad (6)$$

Where g(x,y) is the enhanced image and 'k' is an experimentally determined constant. The optimal value of 'k' was 0.45. For this particular value, the holes in the ridges were filled up. Above 0.45, false joining of ridges was seen to occur. The Inverse Fourier Transform which gives back the image in the spatial domain was obtained using (7).

$$f(x,y) = \frac{1}{MN} \sum_{x=0}^{M-1} \sum_{y=0}^{N-1} F(u,v) \exp\{j2\Pi[\frac{ux}{M} + \frac{vy}{N}]\} \quad (7)$$

To improve the overall contrast of the fingerprint image, FFT enhancement was followed by Histogram Equalisation and the final enhanced image is as seen in Fig 11.

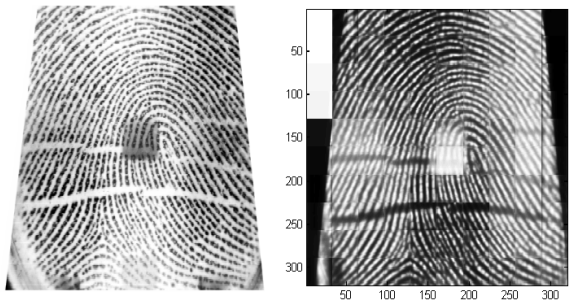

FIGURE 11: (a) Original Image **(b)** Enhanced Image

It could be seen that there are unwanted information at the boundaries of the fingerprint image. Hence the image had to be segmented to extract the region with maximum information. Before segmentation, the image was binarised as seen in Fig 12. The binarisation method adopted was a locally adaptive binarisation method where the mean intensity value of every 16 x 16 block was calculated and based on it, every pixel value in the block was transformed to 1 if its intensity was greater than the mean and made to be zero, if its intensity value was less than the mean. Now, in the image, the ridges are black and the furrows are white so that it is easy to discern the terminations and bifurcations.

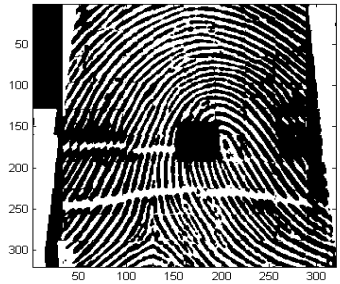

FIGURE 12: Binarised Image

Segmentation of the background from the rest of the image was carried out as a two step process: First, the direction of each 16 x 16 block was estimated. Since the background would have the minimum number of ridges and furrows, it would have the minimum gradient. The gradient in both 'x' and 'y' directions, namely gx and gy were calculated for each block using the Sobel filter, whose masks are: [1 2 1;0 0 0;-1 -2 -1] and its transpose. The certainty level of each block was calculated using (8). The blocks with certainty level

$$E = \{2\sum\sum(gx * gy) + \sum\sum(gx^2 - gy^2)\}/W * W * \sum\sum(gx^2 + gy^2) \qquad (8)$$

Below 0.05 were segmented out as background as seen in Fig 13(a).

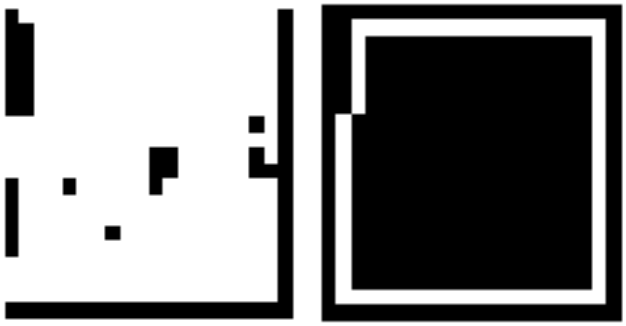

FIGURE 13: (a) Background Blocks **(b)** Morphologically Transformed Image

The background blocks are seen at the boundary as well as inside the image. The blocks inside the image were eliminated using the morphological operations Dilation followed by Erosion as seen in Fig 13(b)

To obtain the region of interest, we propose a method of ROI extraction, where, from the set of columns of pixels with information greater than zero, the column with minimum information is chosen to be the leftmost column of the area of interest and the column with maximum information becomes the rightmost column. The transpose of the image is taken and same process is repeated to get the top and bottom of the ROI as seen in Fig 14 (a). The ROI was multiplied with the binarised image to get the binarised ROI as seen in Fig 14(b). The next step in the process was skeletonising the image. The binarised RoI was reduced to a single pixel thickness by a thinning process. This is essential to mark accurately the minutia points. The thinned image is shown in Fig 15(a).

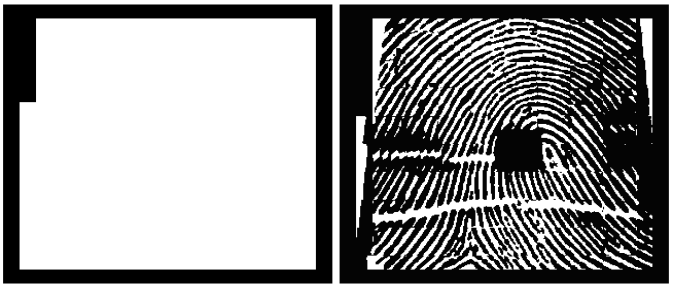

FIGURE 14: (a) ROI Boundary **(b)** ROI in Image

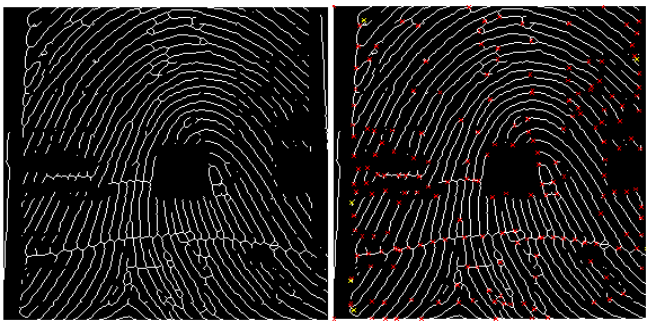

FIGURE 15: (a) Thinned Image **(b)** Minutia Points

The termination points and bifurcation points on the ridges are called minutiae. However false ridge breaks and false ridge cross connections would result in false minutiae. To remove these points, the inter ridge width was calculated and the termination and bifurcation points on the same ridge separated by the inter ridge distance were removed. The minutia were extracted using the method proposed by Sojka, similar to the extraction process used for vein images. The minutia points are marked in Fig 15(b). Fig 16 shows the distribution of the x, y, θ values of the minutia points of two persons.

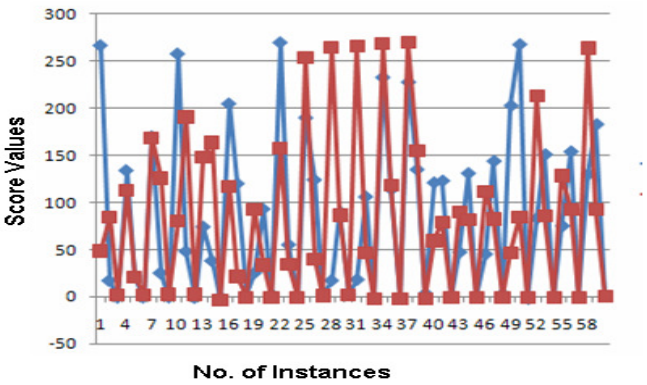

FIGURE 16: Minutiae Distribution for two persons

It can be seen that they are unique to some extent. In order to compare with the hand vein we obtained the cross correlation plot of the fingerprint which is shown in Fig 17.

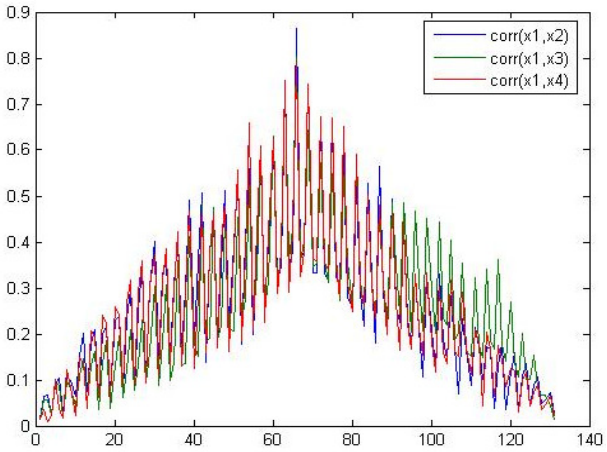

FIGURE 17: Cross Correlation Plot of Fingerprint

Comparing Fig 8 and Fig 17, we see that the correlation or similarity is more between hand veins than the fingerprint. Even though there are various advantages such as spoof-resistance, contactless acquisition, etc., the randomness and hence the accuracy of the hand vein system is low. This is due to the low cost imaging setup we have used which fails to capture a few veins that do not appear prominent enough. Hence to improve the randomness with the same imaging setup, we propose a fusion method.

6. EVALUATION OF MULTIMODAL SYSTEM

To increase the randomness of the hand vein feature vector, we propose addition of more information to it, by fusing yet another feature set, namely the statistical data.

Each feature vector can be considered as a random variable and the distribution of the feature vectors taken at ten different instances with the same subject, as a random process. Moments are calculated for all the seventy-four random processes. In our paper we have used seven invariable moments as proposed by Hu, to describe each random variable, namely the feature vector. For a discrete image f (i,j), of size M x N, its geometry moment in p+q ranks, where p,q are constants can be defined as in (9).

$$M_{pq} = \sum_{i=1}^{M} \sum_{j=1}^{N} i^p j^q f(i, j)$$
$$i \in M, j \in N \qquad (9)$$
$$Set\ \mu_{pq} = \frac{M_{pq}}{M^r}, r = \frac{(p + q + 2)}{2}$$

The 7 absolute moments which are rotation scaling and translation invariant are taken as given by (10)

$$M_1 = \mu_{20} + \mu_{02}$$
$$M_2 = (\mu_{20} - \mu_{02})^2 + 4\mu^2_{11}$$
$$M_3 = (\mu_{30} - 3\mu_{12})^2 + (3\mu_{21} - \mu_{03})^2$$
$$M_4 = (\mu_{30} + \mu_{12})^2 + (\mu_{21} + \mu_{03})^2$$
$$M_5 = (\mu_{30} - 3\mu_{12})(\mu_{30} + \mu_{12})[\mu_{30} + \mu_{12})^2 - 3(\mu_{21} + \mu_{03})^2]$$
$$+ (3\mu_{21} - \mu_{03})(\mu_{21} + \mu_{03})[3(\mu_{30} + \mu_{12})^2 - (\mu_{21} + \mu_{03})^2 \qquad (10)$$
$$M_6 = (\mu_{20} - \mu_{02})[(\mu_{30} + \mu_{12})^2 - (\mu_{21} + \mu_{03})\ ] +$$
$$4\mu_{11}(\mu_{30} + \mu_{12})^2(\mu_{21} + \mu_{03})$$
$$M_7 = (3\mu_{12} - \mu_{03})(\mu_{30} + \mu_{12})[(\mu_{30} + \mu_{12)})^2 - 3(\mu_{21} + \mu_{03})^2]$$
$$+ (\mu_{30} - 3\mu_{12})(\mu_{21} + \mu_{03})[3(\mu_{30} + \mu_{12})^2 - (\mu_{21} + \mu_{03})^2]$$

The moments take on values for one instance of a person as follows for example: 19.61538, 381.7633, 383.7633, 769.5266, 592171.2, 296085.6, -592171. The distribution of moments for 5 different instances of the same person is shown in Fig 18.

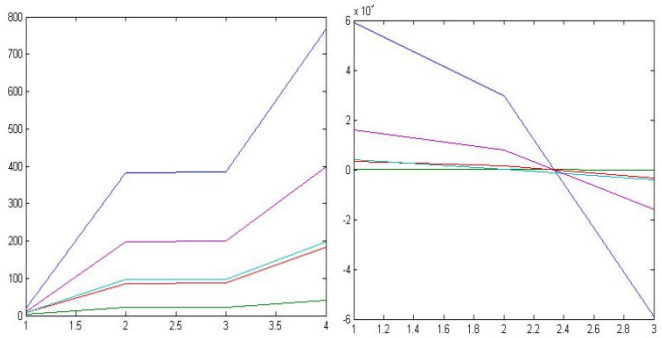

FIGURE 18: Moments M1, M2, M3, M4 and M5, M6, M7

It can be seen the moments calculated are indeed rotation, scaling and shift invariant. The feature vectors created using the two different feature extraction algorithms are fused to form a single feature vector. It can be seen from the distributions that the minutia points and moments are entirely two different entities with different nature and different distributions in space. Being totally independent modalities, these two data sets, when fused give a feature vector whose randomness is further increased, this in turn enhances the accuracy of the system. This was verified by again observing the cross correlation between the fused feature vectors as shown in Fig 19

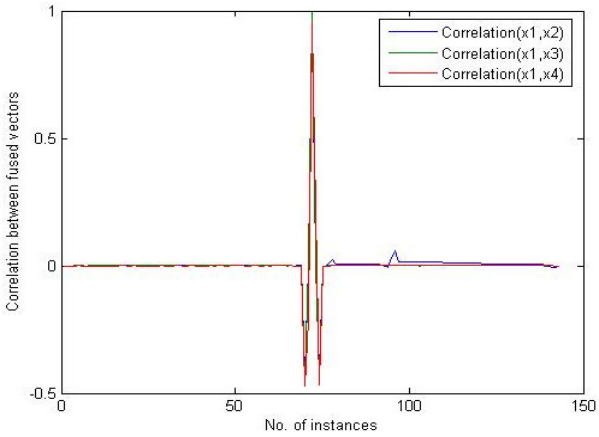

FIGURE 19: Cross correlation among Fused Vectors of the Hand Veins

It can be seen that the variation between different subjects is more, or the correlation is less when the pattern classification is done using the fused vectors. Hence we consider only the feature vectors created by concatenating the morphological data and statistical data, for identification and now the system is said to be multimodal.

To compare the performance scores of the Hand vein and Fingerprint systems, it was necessary to create a fingerprint database. Using the same volunteer crew of 74 persons from whom we obtained the hand veins, we obtained the fingerprint images. Ten instances of fingerprints are stored for each person. For calculating the score, for each person, five are taken as the standard set and five are taken as the testing set. The similarity between the standard images and the test images was measured using the Euclidean Distance Metric. Euclidean distance classifier uses genuine and imposter score for classification. The genuine score is generated by calculating the Euclidean Distance between the testing set and the standard set of the same individual. Same procedure is followed for all the individuals in the database. The distance will be less between the various instances of the same persons. Thus the total count of genuine score is 74x5x5=1850.

Imposter score is generated by calculating the Euclidean distance between a person's testing set and the standard set of all other members. It is repeated for all individuals. Thus the total count of imposter score is 370x365=135050.

A Threshold is set based on the genuine and imposter scores. If the Euclidean distance calculated is less than the threshold, they are recognized as genuine persons. If the score is greater than the threshold, the person is recognized as an imposter. The genuine and imposter scores are shown in Fig 20(a) and (b) respectively.

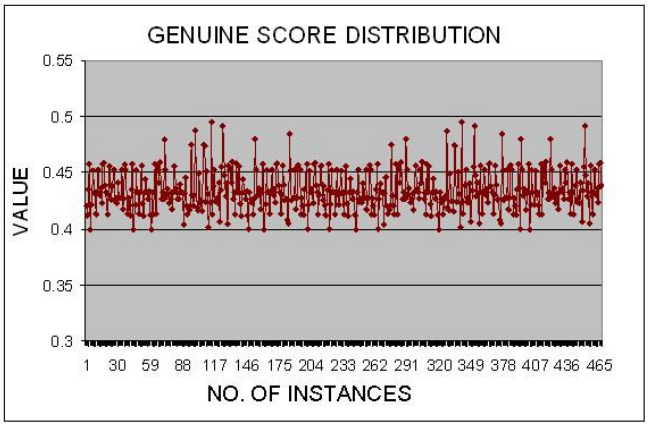

FIGURE 20 (a): Genuine Score Distribution of Fingerprint

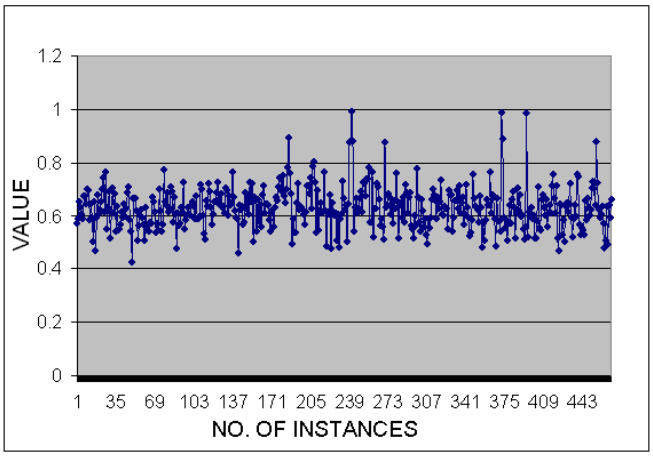

FIGURE 20 (b): Imposter Score Distribution of Fingerprint

The Euclidean distances between the input feature vector and those in the database are calculated using (11)

$$W(k) = \sum [(f_{iw} - f^{k}{}_{iw})^2 / (\delta^{k}{}_{iw})^2] \qquad (11)$$

Where, f_{iw} is the 'i'th feature of the input feature vector and f_{iw}^{k} is the 'i'th feature of the template feature vector in the database, δ_{iw}^{k} is the standard deviation of the template set.
If the distance between the input vector and the vectors in class 'k' are less than a threshold, then the input hand vein is classified as the 'k'th class.

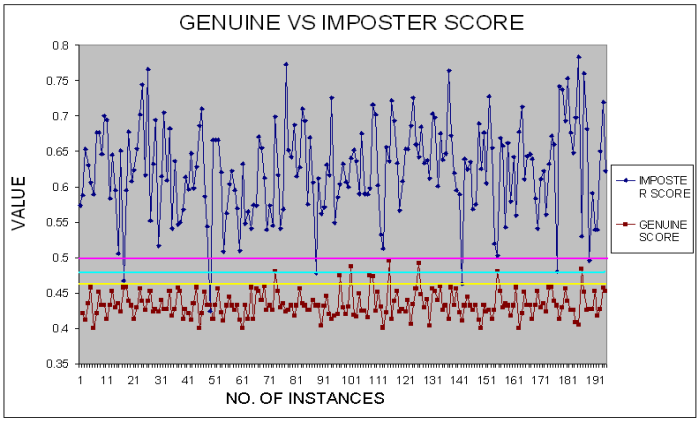

FIGURE 21: Genuine Vs Imposter Scores for Fingerprint

It can be seen in Fig 21 that the genuine score and imposter score overlap at certain points. Hence an optimal threshold is chosen so that, if the match score is less than the threshold, the person is recognized as a genuine user and if greater than the threshold, the person is recognized as an imposter. The case where a true user is considered as an imposter and rejected is called false rejection; and the case where an imposter is recognized as a true user is called false acceptance. The False Acceptance Rate (FAR) and the False Rejection Rate (FRR) vary according to the threshold chosen as seen in Table 2.

Threshold	FAR(%)	FRR(%)
0.5	2.02	1.4
0.475	**1.2**	**1.52**
0.46	0.9	2.7

TABLE 2: Determination of FAR and FRR for Fingerprint

The threshold is chosen to be 0.475, since it has optimal FAR and FRR. Similarly the genuine and imposter scores of the hand vein pattern were calculated for the fused vectors and are shown in Fig 22(a) and (b).

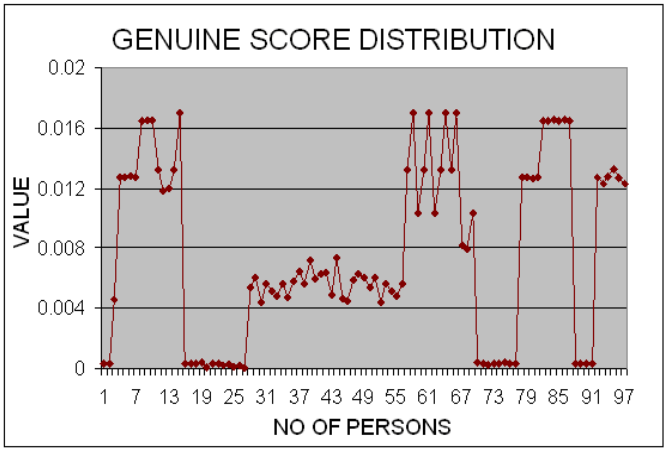

FIGURE 22(a): Genuine score Distribution for Hand Veins

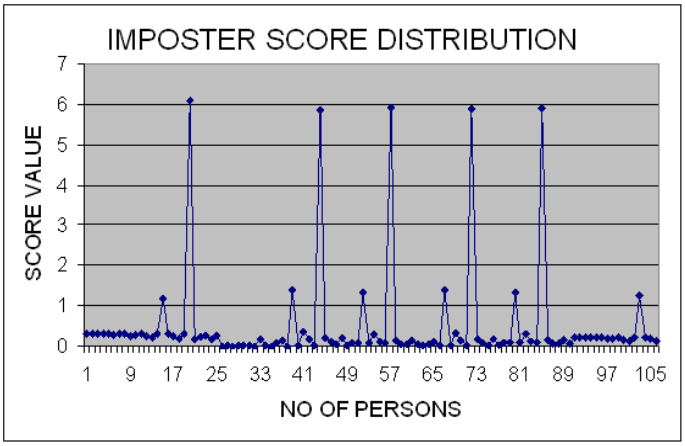

FIGURE 22(b): Imposter score Distribution for Hand Veins

From the genuine and imposter scores we fixed the threshold to be 0.01, where we had minimum overlapping of both the distributions. With this threshold, we obtained an FAR of 0.7 and FRR of 0.46.

It can be seen that the hand vein system with fused feature vectors performs much better than the fingerprint. Another type of multi-biometric system is one which fuses the feature sets of two different biometric modalities and is called a multbiometric system. Section VII discusses the performance of the multibiometric system which fuses the hand vein and fingerprint features.

7. Evaluation of Multi-Biometric System

Here the fusion was done by concatenating the feature set of vein and fingerprint. Let X= {x1, x2…xm} and Y= {y1, y2…yn} denote the feature vector representing the information extracted from vein and fingerprint respectively. Vector Z is formed by concatenation of these two feature sets. However the two feature sets had widely varying range and scale of values. Hence normalization was done to the feature vector before concatenation, to ensure that they are in the same range and scales of values. Min-max normalization performs a linear transformation on the original data. Suppose that min and max are the minimum and the maximum values for attribute A. Min-max normalization preserves the relationships among the original data values. It maps a value v of A to new_v in the range [new-min, new-max] by computing new_v as seen in (12)

$$new\_v = \frac{v - \min_x}{\max_x - \min_x}.(new\_\max_x - new\_\min_x) + new\_\min_x \qquad (12)$$

Let X_{norm} and Y_{norm} represent the normalized feature sets of vein and fingerprint. These features are then concatenated into a single feature set as concat= (X_{1norm}… X_{2norm} ……Xm_{norm} ...$Y_{1\ norm}$, $Y_{2\ norm}$, ……Yn_{norm}). The resultant vector was not of an optimal length. Hence the redundant features in the fused set were removed using "K-means" clustering techniques, which choose the most proximate feature to the mean of the cluster.

Similar to the previous case, the Imposter and Genuine scores were calculated and are shown in Fig 23 (a) and (b).

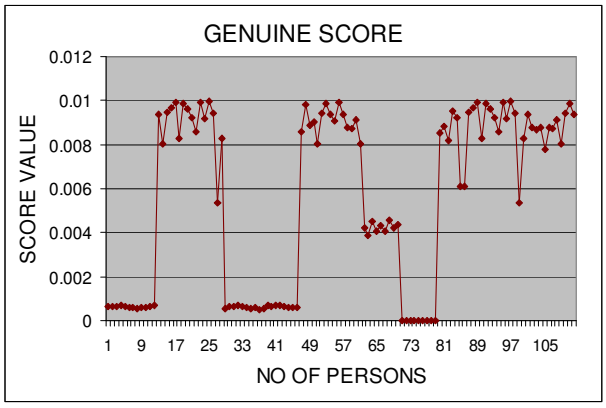

FIGURE 23(a): Genuine Score Distribution for Fingerprint-Hand Vein System

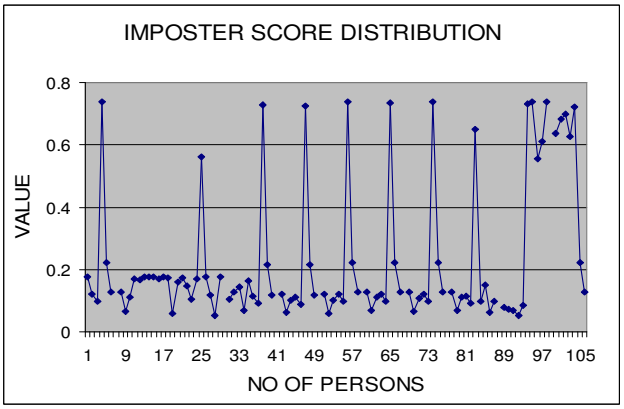

FIGURE 23(b): Imposter Score Distribution for Fingerprint-Hand Vein System

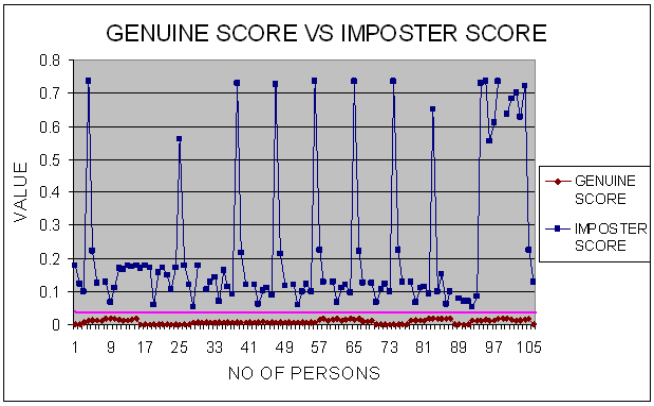

FIGURE 24: Genuine Score vs. Imposter Score for the Fingerprint-Hand Vein System

With the threshold of 0.03, obtained from Fig 24, an FRR of 0% and FAR of 0.01% were obtained for the Fingerprint-Hand vein system.

Biometric System	FAR(%)	FRR(%)
Fingerprint	4.81	2.07
Multimodal Hand Vein System	0.46	0.7
Multi-biometric Fingerprint-Hand Vein System	0	0.01

TABLE 3: Comparison of proposed Biometric Systems

Reference	Methodology	Imaging	Database	Performance
T. Tanaka and N.Kubo [15]	FFT based phase correlation	Near Infra Red, HDF	25 Users	FAR – 0.73% FRR – 4%
C. L. Lin and K. C. Fan [12]	Multi-resolution analysis and combination	Thermal Handvein Imaging	32 Users	FAR – 1.5% FRR – 3.5%
L. Wing and G. Leedham [23]	Line Segment Hausdorff distance matching	Thermal Hand Vein Imaging	12 Users	FAR – 0% FRR – 0%
Y. Ding, D. Zhuang and K. Wang [24]	Distance between feature points	Near IR Imaging, HDF	48 Users	FAR – 0% FRR – 0.9%
J. M. Cross and C. L. Smith [25]	Sequential Correlation in Vein maps	Near IR Imaging, HDF	20 Users	FAR – 0% FRR – 7.9%
A. Kumar and K.Venkata Prathyusha [16]	Matching vein triangulation and shape features	Near IR Imaging Contactless	100 Users	FAR – 1.14% FRR – 1.14%
Proposed Fingerprint-Hand Vein Multi-biometric System	Extraction and Fusion of highly random feature sets to improve performance	Near IR Imaging & Optical Fingerprint Sensor	74 Users	FAR –0 % FRR – 0.01%

TABLE 4: Comparative Summary of available literature on Hand Vein (Back Surface) Based Authentication

8. CONCLUSION AND DISCUSSIONS

From our detailed literature survey on Biometrics in general, we find that the Hand Veins have better circumvention. They can also be obtained equally for peoples of all skin colors. The Multimodal Handvein system is a contactless and hence hygienic biometric identification system suitable for hospitals. It gives a fairly good performance with FAR of 0.46 and FRR of 0.7. A choice of an even more high performance system is suggested in this paper, namely, a multi-biometric system. In situations where hygiene can be compromised for increased accuracy, the multi-biometric system which uses fingerprint and hand veins can be used. This system gives an FAR of 0% and FRR of 0.01%. Further hand vein and fingerprint are traits which are very less prone to damage even in critical cases like accidents. It can also be easily acquired without much patient cooperation. Thus the proposed multi-biometric system using fingerprint and hand vein is ideal for use in healthcare environments.

Increasing the randomness of the biometric template is proposed in this paper for improving the accuracy of the system. As discussed in the earlier sections, when the constituents of a feature vector are highly independent of each other, the randomness of the vector increases. The feature vectors used in the proposed fingerprint-handvein multibiometric system, comprise of the statistical and morphological feature sets of the handvein which are highly independent of each other.

There are several citations in literature that biometric systems based on multiple biometrics are more accurate than systems which depend on a single biometric. As seen in the earlier discussions, hand vein is a biometric identifier whose circumvention is much appreciated than other biometric traits and hence has an inherent quality of high randomness. The performance of the hand vein system can be improved by supplementing it with another biometric. Fingerprint is a very popular, proven, cost effective technology. Hence we have fused the fingerprint with hand vein to create the feature vector which in turn further increases the randomness of the template and hence the performance of the system. The fusion of multiple feature sets as well as multiple biometrics have led to a very remarkable performance rates, namely the FAR of 0% and FRR of 0.01%

9. ACKNOWLEDGEMENT

The author thanks the Management of PSG College of Technology for the facilities and support extended. The author also thanks the staff and student members of the Biomedical Engineering and ECE departments of the same college for their cooperation.

10. REFERENCES

1. http://www.cesg.gov.uk/site/ast/biometrics/media/Biometric/SecurityConcerns.pdf

2. A K Jain, A Ross, and S Pankanti. *"Biometrics: A Tool for Information Security"*. IEEE Transactions on Information Forensics and Security, 1(2):125-143, 2006

3. Nandakumar, K. *"Multibiometric Systems: Fusion Strategies and Template Security"* Doctor of Philosophy, Michigan State University, 2008

4. Uludag U., Ross A., Jain A.K. *"Biometric Template Selection and Update: A Case Study in Fingerprints"*. Pattern Recognition, 37(7):1533-1542, 2004

5. Dass S.C, Jain A.K.. *"Fingerprint Based Recognition"*. Technometrics, Technometrics, 49(3):262–276, 2007

6. Wuzhili. *"Fingerprint Recognition"*. Doctor of Philosophy, Hong Kong Baptist University, 2002

7. Kaur M, M Singh, A. Girdhar, and P. Sandhu. *"Fingerprint Verification System using Minutiae Extraction Technique"*. Proceedings of World Academy of Science, Engineering and Technology, 36: 2008

8. E Sojka. "*A New and Efficient Algorithm for Detecting the Corners in Digital Images*". Pattern Recognition, Luc Van Gool (Editor), LNCS 2449:125-132, 2002

9. Z Zhang, S Ma, X Han. "*Multiscale Feature Extraction of Finger-Vein Patterns Based on Curvelets and Local Interconnection Structure Neural Network".* Proceedings of the 18th International Conference on Pattern Recognition (ICPR '06), Hong kong, 2006

10. J Hashimoto Information & Telecommunication Systems Group, Hitachi, Ltd. *"Finger Vein Authentication Technology and its Future".* Symposium on VLSI Circuits Digest of Technical Papers, 2006

11. N Miura, A. Nagasaka, and T Miyatake. *"Feature Extraction of Finger-Vein Patterns Based on Repeated Line Tracking and its Application to Personal Identification"*. Machine Vision and Applications, 15(4):194-203, 2004

12. C Lin. and K Fan. *"Biometric Verification Using Thermal Images of Palm Dorsa Vein Patterns"*. IEEE Transactions on Circuits and systems for Video Technology, 14(2):188-195, 2004

13. J Cross and C Smith. *"Thermo graphic Imaging of the Subcutaneous Vascular Network of the Back of the Hand for Biometric Identification"*. Proceedings of 29th International Carnahan Conference on Security Technology, Institute of Electrical and Electronics Engineers, Sanderstead, 20–35, 2009

14. S Im, H Park, Y Kim, S Han, S Kim, C Kang, and C Chung. *"A Biometric Identification System by Extracting Hand Vein Patterns"*. Journal of the Korean Physical Society, 38(3):268-272, 2001

15. T Tanaka and N Kubo. *"Biometric Authentication by Hand Vein Patterns"*. SICE, Annual Conference 249-253, Sapporo, August 2004

16. A Kumar, K Prathyusha. *"Personal Authentication Using Hand Vein Triangulation and Knuckle Shape"*. IEEE Transactionss on Image Processing, 18(9):2127-2136, 2009

17. M Shahin, A. Badawi, M Kamel. *"Biometric Authentication using Fast Correlation of Near Infrared hand vein patterns"*. International Journal of Biomedical sciences, 2(3): 2007

18. T Ko. *"Multimodal Biometric Identification for Large User Population using Fingerprint"*. Face and Iris Recognition, Proceedings of the 34th Applied Imagery and Pattern Recognition Workshop (AIPR05), Washington, DC, 2005

19. K Wang, Y Zhang, Z Yuan and D Zhuang. *"Hand Vein Recognition based on Multi supplemental features of multi-classifier fusion decision"*. Proceedings of the IEEE International Conference on Mechatronics and Automation, Luoyang, Henan, June 2006

20. Jain, Bolle R., and S. Pankanti. *"Biometrics: PersonalIdentification In Networked Society"*. Kluwer Academic Publishers, Dordrecht, 1999

21. W LingYu, G Leedham. *"Near and Far Infrared Imaging for Vein Pattern Biometrics*". Proceedings of the IEEE International Conference on Video and Signal Based Surveillance (AVSS'06), Sydney, Australia, 2006

22. [22] J Duncombe. "*Infrared navigation—Part I: An assessment of feasibility (Periodical style)"*. IEEE Trans. Electron Devices, 11:34–39, 1959

23. L Wang and G Leedham. *"A thermal hand-vein pattern verification system".* Pattern Recognition and Image Analysis, Springer, 3687:58–65, 2005

24. Y Ding, D Zhuang and K Wang. *"A study of hand vein recognition method"*. Proceedings of IEEE International Conference on Mechatronics & Automation, Niagara Falls, Canada, 2106-2110. Jul. 2005

25. J Cross, and C Smith. *"Thermo graphic imaging of the subcutaneous vascular network of the back of the hand for biometric identification"*. Proc. IEEE 29th Annu. Int. Carnahan Conf. Security Technology, Sander-Stead, Surrey, U.K, 20–35, 1995